Impact of age-associated increase in 2′-O-methylation of miRNAs on aging and neurodegeneration in Drosophila

Masashi Abe,[1] Ammar Naqvi,[2] Gert-Jan Hendriks,[1,3] Virzhiniya Feltzin,[1] Yongqing Zhu,[1] Andrey Grigoriev,[2,4] and Nancy M. Bonini[1,4]

[1]Department of Biology, University of Pennsylvania, Philadelphia, Pennsylvania 19104, USA; [2]Department of Biology, Center for Computational and Integrative Biology, Rutgers University, Camden, New Jersey 08102, USA

MicroRNAs (miRNAs) are 20- to ~24-nucleotide (nt) small RNAs that impact a variety of biological processes, from development to age-associated events. To study the role of miRNAs in aging, studies have profiled the levels of miRNAs with time. However, evidence suggests that miRNAs show heterogeneity in length and sequence in different biological contexts. Here, by examining the expression pattern of miRNAs by Northern blot analysis, we found that *Drosophila* miRNAs show distinct isoform pattern changes with age. Surprisingly, an increase of some miRNAs reflects increased 2′-O-methylation of select isoforms. Small RNA deep sequencing revealed a global increase of miRNAs loaded into Ago2, but not into Ago1, with age. Our data suggest increased loading of miRNAs into Ago2, but not Ago1, with age, indicating a mechanism for differential loading of miRNAs with age between Ago1 and Ago2. Mutations in *Hen1* and *Ago2*, which lack 2′-O-methylation of miRNAs, result in accelerated neurodegeneration and shorter life span, suggesting a potential impact of the age-associated increase of 2′-O-methylation of small RNAs on age-associated processes. Our study highlights that miRNA 2′-O-methylation at the 3′ end is modulated by differential partitioning of miRNAs between Ago1 and Ago2 with age and that this process, along with other functions of Ago2, might impact age-associated events in *Drosophila*.

MicroRNAs (miRNAs) are 20- to 24-nucleotide (nt) small RNAs that regulate gene expression post-transcriptionally through translational repression and/or mRNA cleavage. Starting from the discovery of the first miRNA lin-4 in *Caenorhabditis elegans*, hundreds of miRNAs have now been identified in various species. miRNAs were classically studied for their role in developmental timing (Lee et al. 1993; Reinhart et al. 2000; Bartel 2004). By now, functional analyses have identified some miRNAs, such as lin-4 in *C. elegans* (Boehm and Slack 2005; Kenyon 2010; Smith-Vikos and Slack 2012) and miR-34 in *Drosophila* (Liu et al. 2012), as miRNAs with critical roles in organismal and brain aging, respectively. Although most studies have focused on changes in the abundance of miRNAs with age (Ibanez-Ventoso et al. 2006; de Lencastre et al. 2010; Kato et al. 2011), evidence

suggests that miRNAs also show heterogeneity in length and sequence in different cell types and biological contexts (Burroughs et al. 2010; Marti et al. 2010; Li et al. 2012; Westholm et al. 2012; Llorens et al. 2013). Such heterogeneity is mediated by imprecise Drosha and Dicer cleavages (Calabrese et al. 2007; Azuma-Mukai et al. 2008; Wyman et al. 2011), 3′ end adenylation/uridylation (Ruby et al. 2006; Landgraf et al. 2007; Burroughs et al. 2010; Wyman et al. 2011), and RNA-editing events (Kawahara et al. 2007; Nishikura 2010; Alon et al. 2012; Ekdahl et al. 2012). Importantly, effects of this heterogeneity on miRNA target silencing are also reported (Azuma-Mukai et al. 2008; Seitz et al. 2008; Fukunaga et al. 2012; Lee and Doudna 2012), suggesting a functional impact of regulating miRNA heterogeneity in animals. Our study on the role of miR-34 in aging and age-

[3]Present address: Friedrich Miescher Institute for Biomedical Research, Maulbeerstrasse 66, 4058 Basel, Switzerland
[4]Corresponding authors
E-mail nbonini@sas.upenn.edu
E-mail agrigoriev@camden.rutgers.edu
Article is online at http://www.genesdev.org/cgi/doi/10.1101/gad.226654.113.

associated neurodegeneration in *Drosophila* revealed an intriguing pattern of miR-34 isoforms: Although multiple-length isoforms of miR-34 are generated, only the short isoform accumulates with age (Liu et al. 2012). Furthermore, the generation of isoforms of miR-34 requires 3′ end trimming by a novel 3′-to-5′ exonuclease, Nibbler (Nbr) (Han et al. 2011; Liu et al. 2011), highlighting the potential importance of regulation of miRNA length in age-associated processes.

In addition to length and sequence heterogeneity, the 2′-OH of the 3′ terminal ribose of miRNAs can be modified by 2′-*O*-methylation (Zhao et al. 2012a). In plants, this modification occurs on nearly all miRNAs and siRNAs (Yu et al. 2005; Zhao et al. 2012a,b) and protects the small RNAs from HESO1-mediated uridylation and degradation (Li et al. 2005; Yu et al. 2005; Ren et al. 2012; Zhao et al. 2012b). In *Drosophila*, most miRNAs are loaded into Ago1 and remain unmodified (Hutvagner et al. 2001; Okamura et al. 2004; Vagin et al. 2006). However, a subset of miRNAs are found to be 2′-*O*-methylated (Forstemann et al. 2007; Horwich et al. 2007; Ghildiyal et al. 2008; Czech et al. 2009; Okamura et al. 2009). Importantly, this modification is also protective in animals: Loss of 2′-*O*-methylation of small RNAs leads to destabilization as well as tailing and trimming of the small RNAs (Kurth and Mochizuki 2009; Ameres et al. 2010; Kamminga et al. 2010).

In *Drosophila*, 2′-*O*-methylation of small RNAs is associated with loading of the miRNAs into different Ago complexes: While most miRNAs are loaded into Ago1 (Ago1-RISC) and remain unmodified, those loaded into Ago2 (Ago2-RISC) are 2′-*O*-methylated (Czech et al. 2009; Okamura et al. 2009; Ghildiyal et al. 2010). The miRNA/miRNA* duplex structure and 5′ nucleotide preference are two suggested mechanisms by which miRNAs are directed into the two distinct Ago complexes (Forstemann et al. 2007; Tomari et al. 2007; Okamura et al. 2009; Ghildiyal et al. 2010). miRNAs loaded into Ago2 are also active in translational silencing of the target genes, like miRNAs loaded into Ago1, but by a potentially different mechanism and with different silencing efficiency (Czech et al. 2009; Iwasaki et al. 2009; Okamura et al. 2009). However, despite the discovery of functional Ago2-loaded and 2′-*O*-methylated miRNAs in *Drosophila*, whether such loading of miRNAs to Ago2 is biologically regulated or biologically important in vivo is not yet clear.

Here, we pursued the study of several Nbr-dependent miRNAs that, like miR-34, show multiple isoforms. Examination of changes in their isoform patterns with age unexpectedly revealed a diversity of patterns. The age-associated increase of some *Drosophila* miRNAs reflected increased 2′-*O*-methylation of select isoforms. Associated with this increase, we found increased loading of specific miRNA isoforms into Ago2, but not Ago1, with age. Furthermore, the lack of 2′-*O*-methylation by *Hen1* and *Ago2* mutations resulted in reduced life span and brain degeneration, raising the possibility that the increased protection of small RNAs with age may impact age-associated events.

Results

Distinct age-associated isoform patterns of Nbr-trimmed miRNAs

Drosophila miR-34-5p, which is a target of Nbr-dependent 3′ end trimming (Han et al. 2011; Liu et al. 2011), shows an increase in the short isoform with age (Fig. 1A,B; Liu et al. 2012). This observation led us to examine the age-associated pattern of other Nbr-trimmed miRNAs. We focused on several miRNAs that could be readily detected by Northern analysis. Northern blots of these miRNAs at 3 d and 30 d in heads revealed intriguing changes in isoform patterns. One Nbr-trimmed miRNA, miR-317-3p, increased with age like miR-34-5p (Fig. 1A,B). The increase in both of these miRNAs reflected an increase in their short isoforms with age. In contrast, although both miR-305-5p and miR-263a-5p increased in total amount with age, their isoform patterns were opposite: These miRNAs showed an increase in the longer isoforms with age (Fig. 1C,D). miR-11-3p showed a single isoform by Northern and increased by 30 d (Fig. 1E,F). These observations raised the possibility that multiple mechanisms are used to generate distinct miRNA isoform patterns with age.

Age-associated increase in 2′-O-methylation of Nbr-trimmed miRNAs

One mechanism to explain an increase in long isoforms with age could be an increased protection of these specific isoforms with age. Almost all plant miRNAs and siRNAs (Li et al. 2005; Yu et al. 2005; Ren et al. 2012; Zhao et al. 2012b) and animal siRNAs and piRNAs are 2′-*O*-methylated (Horwich et al. 2007; Kirino and Mourelatos 2007a,b,c). Recent studies also suggest that a subset of *Drosophila* miRNAs are 2′-*O*-methylated (Forstemann et al. 2007; Horwich et al. 2007; Czech et al. 2009; Okamura et al. 2009; Ghildiyal et al. 2010). Importantly, 2′-*O*-methylation of animal small RNAs is also protective such that loss of 2′-*O*-methylation leads to their destabilization (Ameres et al. 2010; Kamminga et al. 2010). Therefore, we hypothesized that the increase of the long isoforms of miR-305-5p, miR-263a-5p, and miR-11-3p may result from increased protection at the 3′ end of specific isoforms by 2′-*O*-methylation. To address this, we performed oxidation/β-elimination assays on total RNA from 3-d and 30-d wild-type heads and bodies. If the 3′ end ribose of small RNAs is protected by 2′-*O*-methylation, as for piRNAs and siRNAs, those small RNAs cannot react with sodium periodate in the oxidation/β-elimination assay and will not decrease in size. However, if the 3′ end ribose is unmodified, they can react, will be β-eliminated, and will shift down in length (Horwich et al. 2007). Therefore, a change in the mobility of the small RNAs by Northern indicates the presence or absence of a protective modification at the 3′ end. We performed this assay and found that miR-34-5p shifted down in size and thus is not protected at the 3′ end (Fig. 2A, left panel). In contrast, miR-305-5p, miR-263a-5p, and miR-11-3p showed an increase in protection of the long
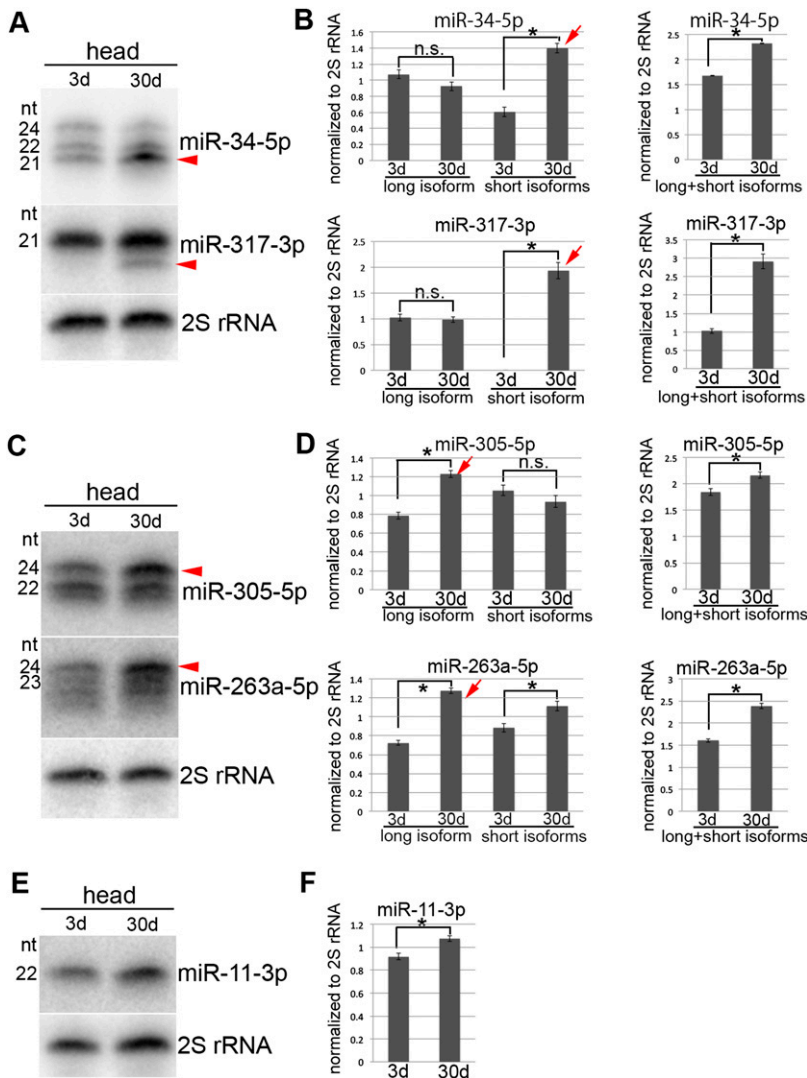
Figure 1. Nbr-dependent miRNAs show distinct isoform patterns with age. Northern blots of different Nbr-dependent miRNAs with age. (*A,B, left* panel) miR-34-5p and miR-317-3p showed accumulation of short isoforms with age. (*B, right* panel) Both miR-34-5p and miR-317-3p also increased in total amount with age. (*C,D, left* panel) miR-305-5p and miR-263a-5p showed accumulation of long isoforms with age. (*D, right* panel) Both miR-305-5p and miR-263a-5p increased in total amount with age. (*E,F*) miR-11-3p, a single-form miRNA by Northern, accumulated with age. (*B,D, left* panels, *F*) Quantification of the different isoforms of each miRNA. (*Right* panels) Quantification of the total amount of each miRNA with age. Red arrowheads and arrows indicate the isoforms that increased with age. Mean ± SD. $n = 3$; (*) $P < 0.05$ (Student's *t*-test).

isoforms with age (Fig. 2A, right panel, arrows). Quantification of the ratio of protected to unprotected isoforms of miR-305-5p, miR-263a-5p, and miR-11-3p showed an increase in the ratio of protected to unprotected isoforms with age. If the increase of the protected isoforms simply reflected an increase of the overall level of these miRNAs, the ratio of protected to unprotected isoforms after oxidation/β-elimination would not change. However, the ratio increased for these three miRNAs (Fig. 2B), indicating a mechanism to increase the protection of the long isoforms of these miRNAs with age.

We next determined whether the protection of specific miRNA isoforms is due to 2′-*O*-methylation at the 3′ end. 2′-*O*-methylation of small RNAs depends on the methyltransferase Hen1. In addition, 2′-*O*-methylation of small RNAs requires loading into Ago2: Loss of Ago2 and Ago2-loading machinery (Dcr2 and R2D2) leads to loss of modification (Horwich et al. 2007). Therefore, to confirm that the miRNAs were 2′-*O*-methylated and loaded into Ago2, we tested the effect of loss of *Hen1* and *Ago2* on the pattern of miR-305-5p, miR-263a-5p, and miR-11-3p with age. *Hen1*[f00810] and *Ago2*[BL16608] mutant flies were aged to

3 d or 30 d, RNA was isolated, and oxidation/β-elimination was performed. This revealed that miR-305-5p, miR-263a-5p, and miR-11-3p were no longer protected but rather depended on *Hen1* and *Ago2* for protection at both 3 d and 30 d (Fig. 3, arrowheads). This finding indicates that the increase of the long isoforms of these miRNAs is dependent on *Hen1* and thus is due to 2′-*O*-methylation at the 3′ end. These data also indicate that these miRNA isoforms are loaded into Ago2 for 2′-*O*-methylation. We note that miR-317-3p is exceptional in that it showed protection of the long isoform from oxidation/β-elimination in both young and old flies (see Fig. 2A, arrowheads); however, to our surprise, protection persisted even after the loss of *Hen1* and *Ago2* (Fig. 3, arrowheads). This suggests that miR-317-3p is protected in a manner independent of *Hen1* and *Ago2* function.

An age-associated increase in Ago2 loading of 2′-O-methylated isoforms of miRNAs

In *Drosophila*, while most miRNAs are loaded into Ago1 and thus are unmodified, a subset of miRNAs has been
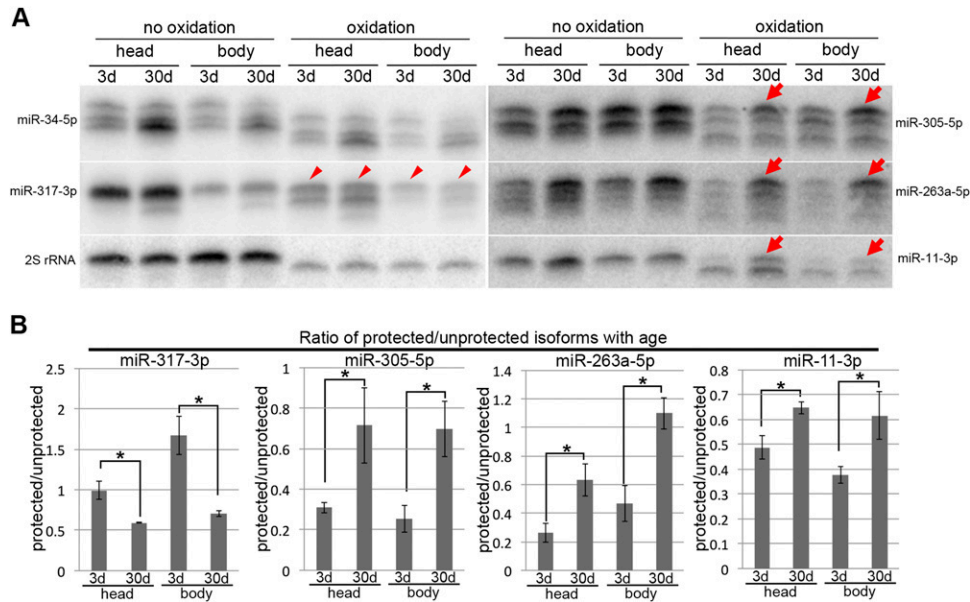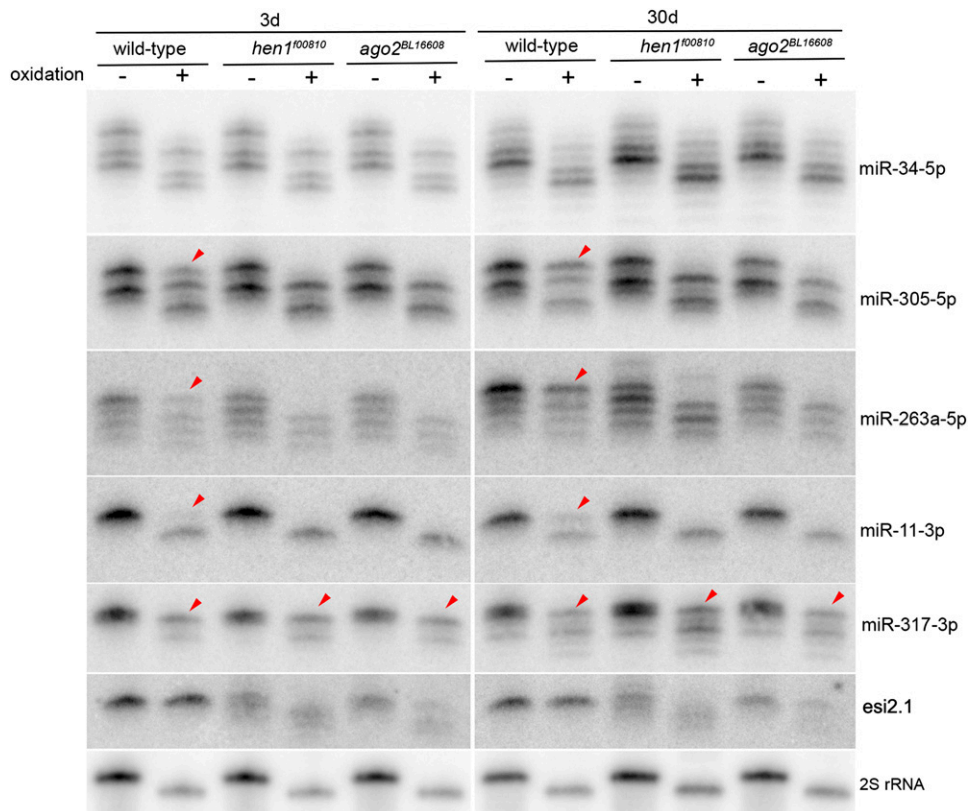
Figure 2. Age-associated increase of long isoforms of miR-305, miR-263a/b, and miR-11 is associated with increased protection from oxidation/β-elimination. Northern blots of miR-305, miR-263a/b, miR-11, miR-34, and miR-317 without (*left* side of each miRNA panel) and with (*right* side of each miRNA panel) treatment by oxidation/β-elimination, with quantitation. (*A*) All isoforms of miR-34 were sensitive to oxidation/β-elimination. The longest isoform of miR-317 was protected (arrowheads), but there was a decrease in the ratio of the protected isoform with age. miR-305, miR-263a/b, and miR-11 show accumulation of a protected long isoform with age (arrows). (*B*) Ratio of oxidation/β-elimination-protected isoforms to unprotected isoforms with age. Mean ± SD. $n = 3$; (⋆) $P < 0.05$ (Student's *t*-test).

observed to be loaded into Ago2 (Ago2-RISC) and is 2′-O-methylated (Czech et al. 2009; Okamura et al. 2009; Ghildiyal et al. 2010). Therefore, based on our findings, we proceeded to determine whether the protected isoforms of miR-305-5p, miR-263a-5p, and miR-11-3p increased their Ago2 loading with age. To do this, we immunoprecipitated Ago1 and Ago2 from whole flies and then performed Northern blots on the precipitated small RNAs, comparing 3 d with 30 d. Ago1 could be immunoprecipitated with an antibody; for Ago2, we used flies bearing a genomically tagged Flag-HA-*Ago2* (Czech et al. 2008). This approach revealed a specific loading pattern for each small RNA with age in Ago1 versus Ago2. miR-34-5p, which was not protected at the 3′ end (see Fig. 2A), was predominantly loaded into Ago1 and was not detectably present in Ago2 (Fig. 4A). Consistent with the age-associated pattern of miR-34-5p by Northern from total RNA (see Fig. 1A; Liu et al. 2012), the short isoforms of miR-34-5p accumulated in Ago1 with age (Fig. 4A). esi-2.1, an abundant endogenous siRNA in flies (Czech et al. 2008; Ghildiyal et al. 2008; Kawamura et al. 2008; Okamura et al. 2008), was selectively loaded into Ago2 and was not detectable in Ago1 (Fig. 4A). In contrast, miR-305-5p and miR-263a-5p showed an intriguing loading pattern: While multiple isoforms were present in Ago1 at both 3 d and 30 d, only the long isoforms (24 nt) were present in Northerns of Ago2-IP material (Fig. 4A). The single isoform of miR-11-3p was present in Ago1; however, a small portion was loaded into Ago2 (Fig. 4A). In addition to the loading of specific lengths of isoforms into Ago2,

there was also a trend of increased levels of the loaded isoforms of miR-305-5p, miR-263a-5p, and miR-11-3p into Ago2 with age. To quantify this, we normalized the level of the Ago2-loaded miRNAs to Ago2-loaded esi-2.1 at the corresponding age; the total level of esi-2.1 did not change with age (Fig. 4B) and is loaded into Ago2 and not into Ago1 (Fig. 4A). After normalizing, we confirmed a significant increase of Ago2-loaded miR-305-5p, miR-263a-5p, and miR-11-3p with age (Fig. 4C–E). These findings suggest that the age-associated increase of 2′-O-methylation of miRNAs reflects increased loading of selective isoforms into Ago2 with age.

One possibility for increased loading into Ago2 could be an increase in the level of Hen1, Ago2, and/or the Ago2-loading machinery (Dcr2 and R2D2) with age (Liu et al. 2003; Tomari et al. 2004; Marques et al. 2010; Okamura et al. 2011; Nishida et al. 2013). To address this possibility, we performed Western immunoblots on Ago2 (Flag-HA-*Ago2* flies), R2D2, and Dcr2 with age (no antibody is available for Hen1). Both Ago2 and R2D2 were unchanged with age (Fig. 4F–H), and Dcr2 was not detectable in adult flies (Supplemental Fig. S1). To further confirm these results, we examined microarray data from aged *Drosophila* brains (3 d, 30 d, and 60 d) (Liu et al. 2012). Analysis confirmed no significant increase in Hen1, Ago2, Dcr-2, or R2D2 RNA levels with age (Supplemental Table S1). In addition, the level of Ago1 mRNA and protein was unchanged, suggesting that a decrease in Ago1 levels would not explain the relative increase in Ago2 loading of miRNAs with age (Supplemental Table S1; Supplemen-

Figure 3. The age-associated increase of the long isoforms of miR-305, miR-263a, and miR-11 is eliminated upon *Hen1* and *Ago2* mutation. Northern blots of each miRNA with or without oxidation/β-elimination at 3 d and 30 d in wild-type, *Hen1^{f00810}*, and *Ago2^{BL16608}* animals. Red arrowheads indicate the isoforms that are protected after oxidation/β-elimination in wild type; these forms for miR-305, miR-263a/b, and miR-11 were no longer protected in *Hen1^{f00810}* and *Ago2^{BL16608}* mutant animals. The long forms of miR-317 remained protected in *Hen1^{f00810}* and *Ago2^{BL16608}* animals, indicating an alternative mechanism by which the long isoform accumulates for this miRNA.

tal Fig. S2). We observed a potential increase in mRNA levels for Hsp70 (Supplemental Table S1), a component of RISC-loading machinery, in a complex with Hsp90 (Iki et al. 2010; Iwasaki et al. 2010; Miyoshi et al. 2010). However, since the Hsp90 level is unchanged, there is likely no increase in the Hsp90/Hsp70 complex with age. Together, these results suggest that the increase of Ago2 loading of miRNAs with age is independent of a change in the level of Ago2 or Ago2-loading machinery.

A global shift of Ago1 vs. Ago2-loaded miRNAs with age

To confirm the increase in miRNA loading into Ago2 with age, we immunopurified Ago1 and Ago2 from flies aged 3 d and 30 d and performed deep sequencing of the small RNA fraction. We normalized the number of observed reads to the total number of non-miRNA reads in Ago1 and to the esi-2.1 reads in Ago2. This analysis showed that the total read number of miRNAs in Ago1 was largely unchanged, while that of Ago2 increased with age (Fig. 5A). In addition, the share of miRNAs among total small RNAs occupying Ago1 showed little change with age, while in Ago2, the miRNA reads increased

dramatically with age (30.7% at 3 d to 69.6% at 30 d) (Fig. 5B). During the analysis, we noticed that miR-263a-5p was the singular most abundant miRNA in the 3-d and 30-d Ago2 libraries. Therefore, to rule out that the increased trend of total miRNA reads and percentage in Ago2 with age simply reflected a change in miR-263a-5p, we also removed miR-263a-5p reads from 3-d and 30-d Ago2-IP libraries and recalculated the total miRNA read number (normalized to esi-2.1) and the percentage of total miRNAs in 3-d and 30-d Ago2 libraries. This confirmed that, even after removing miR-263a-5p, the trend persisted: The read number and percentage of the total miRNAs in Ago2 increased with age (Supplemental Fig. S3). These results, together with the increased ratio of protected to unprotected isoforms of miRNAs with age (see Fig. 2), support the idea that more miRNA molecules are becoming loaded into Ago2, and not Ago1, with age.

We analyzed in detail the three miRNAs that were the focus of Northern analysis: miR-305-5p, miR-263a-5p, and miR-11-3p. Supporting the earlier observations, miR-305-5p, miR-263a-5p, and miR-11-3p showed increased association in Ago2 with age (Fig. 5C, bottom panels). In contrast, the amount of these miRNAs in Ago1 decreased
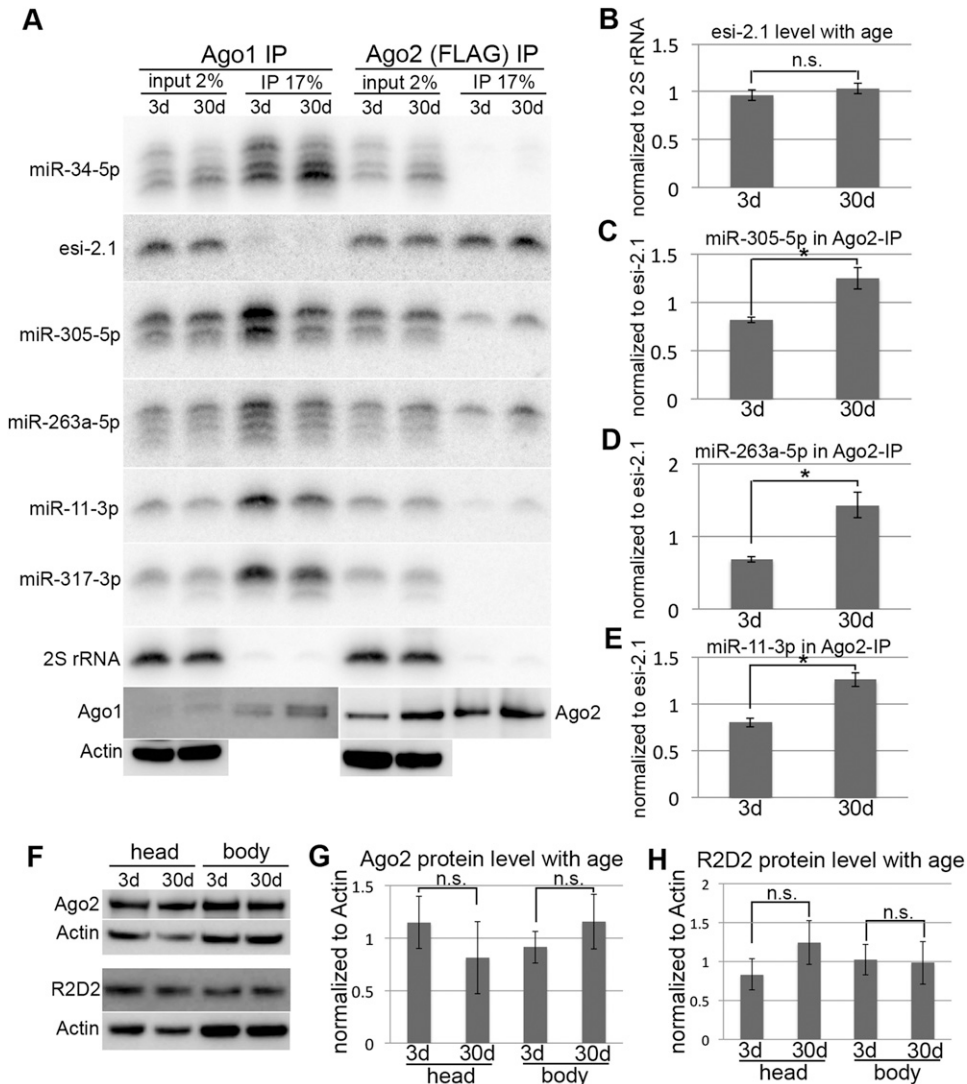
Figure 4. Increased Ago2 loading of long miRNA isoforms with age. Northern blots with quantitation of miRNAs associated with Ago1 versus Ago2 with age. (*A*) Northern blots for small RNAs on RNA isolated from Ago1-IP (*left*) and Ago2-IP (Flag-HA-*Ago2*) (*right*). (*B*) Quantification of esi-2.1 level with age. Mean ± SD. $n = 4$; Student's *t*-test confirmed no significant differences with age. There is no change in esi-2.1 levels with age. (*C*–*E*) Quantification of miRNA isoforms loaded into Ago2 with age, normalized to esi-2.1 in Ago2-IP. Mean ± SD. $n = 3$; (*) $P < 0.05$ (Student's *t*-test). For all three miRNAs, the Ago2-loaded isoforms increase with age. (*F*) Western immunoblot for Ago2 and R2D2 with age. (*G*) Quantification of Ago2 protein level with age. Mean ± SD. $n = 3$; not significant by Student's *t*-test. (*H*) Quantification of R2D2 protein level with age. Mean ± SD. $n = 4$; not significant by Student's *t*-test.

with age (Fig. 5C, top panels). Together, these data support the idea that the loading pattern of miRNAs between Ago1 and Ago2 changes dramatically with age such that Ago2 loading of selective miRNA isoforms increases, while Ago1 loading of the miRNA isoforms generated from the same stem–loops decreases.

Detailed analysis of the libraries allowed identification of additional miRNAs with the same trend of an increase of select isoforms in Ago2 with age. We compared relative loading ratios (Ago2 over Ago1, R_{21}) (see the Materials and Methods) of the most abundant isoform for each miRNA in 30-d flies versus 3-d flies (Fig. 6A). This showed the three miRNAs that were the focus of our tests with Northerns (miR-305-5p, miR-263a-5p, and miR-11-3p) are

among those preferentially loaded into Ago2 at both 3 d and 30 d (Fig. 6A).

Among the 240 *Drosophila* miRNA genes, 135 were detected with at least one raw read in both Ago1-IP and Ago2-IP libraries at 3 d, while 143 were detected at 30 d. Among these, 67 5p and 3p sequences had at least 1000 raw reads of at least one isoform at 3 d or 30 d, of which 15 mature and nine star sequences showed preferential loading of specific isoforms into Ago2 relative to Ago1 at 3 d ($R_{21} > 1.2$), while 16 mature and nine star sequences showed that trend at 30 d ($R_{21} > 1.2$) (Fig. 6A; Supplemental Tables S2, S3). (5p and 3p sequences were classified as "mature" or "star" based on their relative abundance in the Ago1-IP 3-d library and a consistent behavior
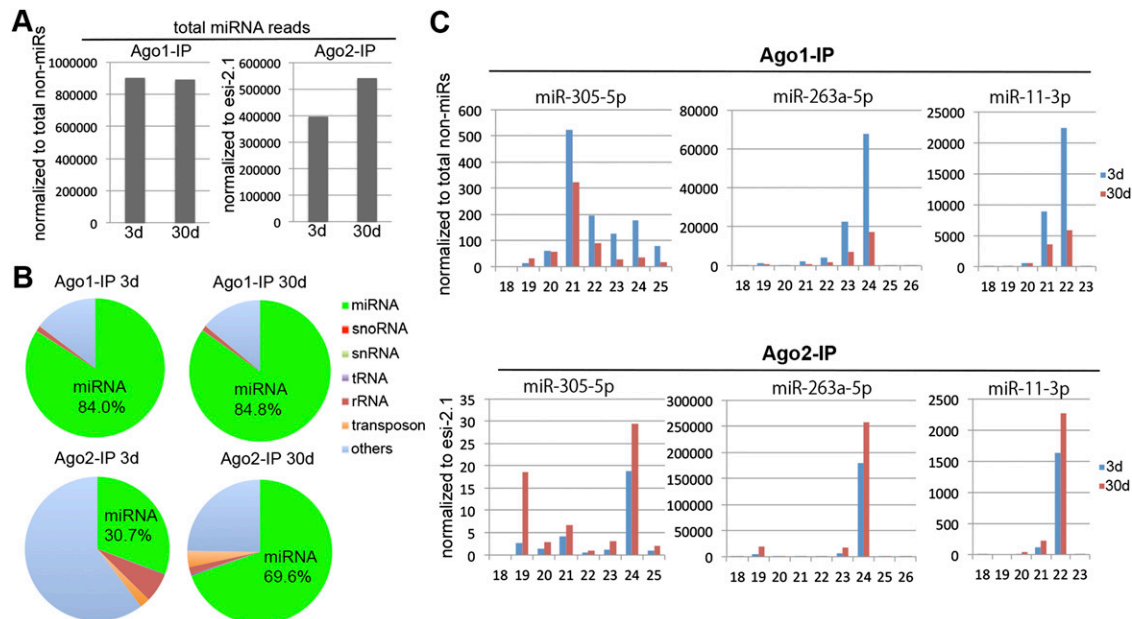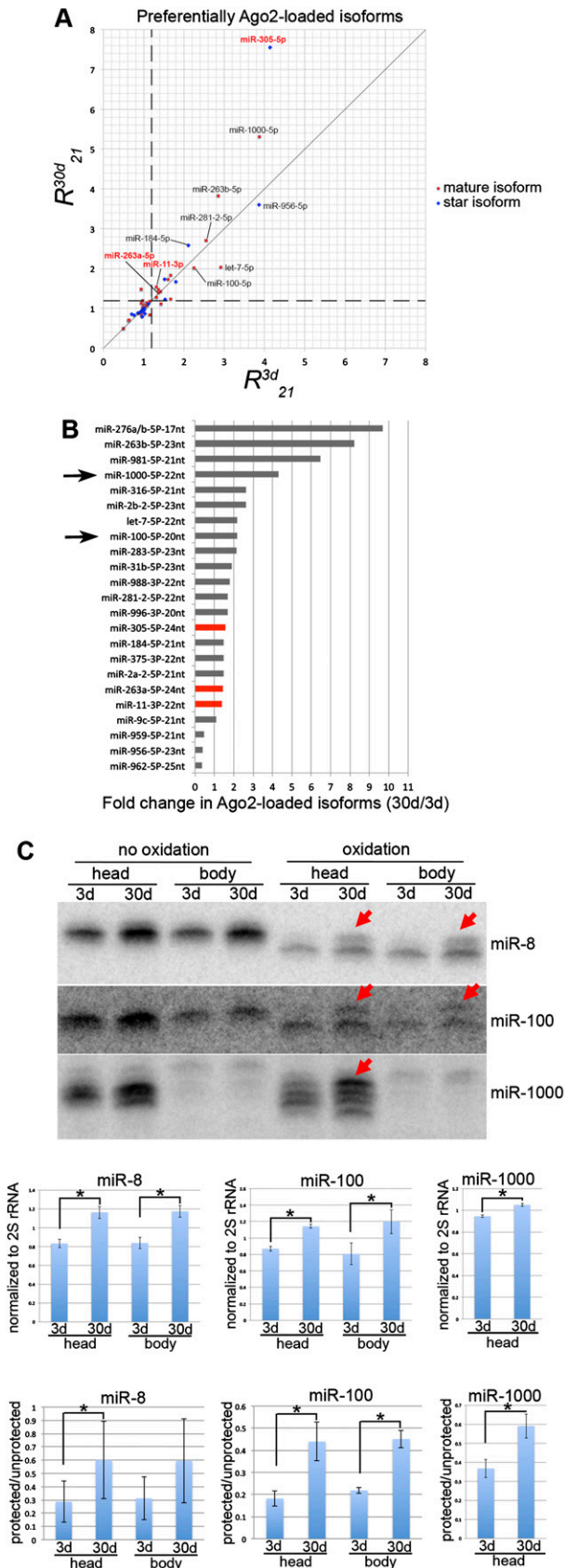
Figure 5. Ago1-IP versus Ago2-IP small RNA deep sequencing with age. (*A*) Normalized read number of total miRNAs in Ago1 or Ago2 with age. (*B*) Percentage of miRNAs and other small RNA classes in Ago1 and Ago2 with age. (*C*) miR-305-5p, miR-263a-5p, and miR-11-3p show a decrease in Ago1 but an increase of specific isoforms in Ago2 with age.

across all four libraries: Those with a higher read number compared with the read number from the other strand of the stem–loop were defined as "mature" [see the Materials and Methods for details].)

Next, we determined whether the miRNA isoforms showing preferential loading into Ago2 compared with Ago1 at either age ($R_{21} > 1.2$ at 3 d or 30 d) (Fig. 6A) also showed an increase in loading into Ago2 with age. To assess the latter value, we calculated for each miRNA the fold change between 30 d and 3 d in normalized read numbers of the main isoform loaded into Ago2 (Fig. 6B). A change of more than one would indicate miRNAs with an increase in specific miRNA loading into Ago2 with age. We confirmed that miR-305-5p, miR-263a-5p, and miR-11-3p showed increased loading into Ago2 with age (Figs. 4A–E, 6B [red bars]). Together, these data indicate that 11 mature and eight star sequences out of 67 (5p and 3p) total sequences with >1000 raw reads of at least one isoform showed preferential loading of specific isoforms into Ago2 relative to Ago1, and such loading increased with age. We also analyzed a library from a previous study comparing Ago1-IP miRNAs to 3′ end-protected miRNA from heads (Ghildiyal et al. 2010). This analysis also indicated a selective enrichment for particular miRNAs (Supplemental Fig. 4). From these analyses (Fig. 6B; Supplemental Fig. 4), we then performed Northern blots on several highlighted miRNAs that would be sufficiently abundant to detect in order to examine whether their protection increases with age: miR-1000, miR-100, and miR-8 (Fig. 6B, black arrows; Supplemental Fig. 4, green bars). Northern blots confirmed accumulation of long isoforms protected at the 3′ end that increased in both level and protected isoforms with age (Fig. 6C).

To gain potential insight into the functional effects of the shift in miRNAs from Ago1 to Ago2 with age, we analyzed gene expression changes in the brain with age, comparing 3 d with 30 d from a previous microarray analysis (Liu et al. 2012). We selected down-regulated and up-regulated genes with high stringency ($P < 0.001$; Benjamini-Hochberg false discovery rate [FDR] < 5%) with expression change (down or up) above twofold. At 30 d versus 3 d, 719 genes were significantly down-regulated, and 199 were significantly up-regulated, giving a global ratio of age-related down-regulation of 3.61 for the whole genome. We then considered the potential effects of miRNAs with increased loading into Ago2 by deep sequencing that were confirmed by Northerns (miR-1000, miR-100, miR-305, miR-11, miR-263a, miR-263b, and miR-8). In a combined list of mRNA targets of these miRNAs (predicted by TargetScan), the down-regulation ratio was substantially higher (104/13 = 8; $P < 0.001$; Benjamini-Hochberg FDR < 5%); thus, these target genes are twice as likely to show stronger down-regulation with age compared with the whole genome. We further analyzed the splicing array data of Taliaferro et al. (2013) following knockdowns of Ago proteins in S2 cells. Although these arrays were designed for quantifying alternative splicing rather than gene expression, they still show trends consistent with our observations. Of 159 deregulated genes with Ago1 knockdown, eight predicted targets of the miRNAs shifted to Ago2 showed changed expression (down-regulated, except for the *cals* gene); all were also down-regulated in the aging microarray at 30 d versus 3 d. Among the 51 deregulated genes in Ago2 knockdown, four predicted targets of the miRNAs shifted to Ago2 showed a change of expression, but it was up-

regulation (except for the *bbc* gene), while they were down-regulated in the aging microarray at 30 d versus 3 d. Thus, for the group of genes in common, there is a striking reversal of expression following Ago2 knockdown, but not Ago1 knockdown, compared with the general down-regulation with age.

Loss of Hen1 and Ago2 is associated with shortened life span and neurodegeneration

To address the biological significance of the global shift in the population of Ago2-loaded miRNAs, we examined the impact of global loss of 2′-O-methylation of small RNAs by analyzing *Hen1* and *Ago2* mutant animals. *Ago2* loss is known to cause defects in synaptic structure in third instar larvae (Pepper et al. 2009), indicating the importance of *Ago2* on neuronal development. Here we focused on adult-specific age-associated effects. Life span analysis indicated that both $Hen1^{f00810}$ and $Ago2^{BL16608}$ mutants showed a shorter life span compared with genetic background-matched controls (Fig. 7D). Detailed analysis of these animals also showed that both $Hen1^{f00810}$ and $Ago2$ ($Ago2^{414}$ and $Ago2^{BL16608}$) mutants have increased brain vacuolization, indicative of brain degeneration with age (Fig. 7A–C). While $Hen1^{f00810}$ mutants showed more brain vacuolization in the optic lamina (Fig. 7B), *Ago2* mutants had excessive vacuoles in the retina (Fig. 7C). Both *Hen1* and *Ago2* mutants are predicted to impact siRNAs, which may contribute to the effects, and the difference in phenotypes between *Hen1* and *Ago2* mutants might reflect a broader role of *Ago2* beyond its effects on siRNAs (Taliaferro et al. 2013). However, defects in both *Hen1* and *Ago2* mutants suggest that 2′-O-methylation of

Figure 6. Identification of Ago2-loaded miRNA isoforms whose loading increases with age. (*A*) Dot plot showing the ratio of preferentially Ago2-loaded isoforms at 3 d (*X*-axis) to 30 d (*Y*-axis). We selected miRNAs with values $R_{21} > 1.2$ as candidates with greater loading into Ago2 at 3 d or 30 d (dashed lines parallel to the axes; miR-305-5p, miR-263a-5p, and miR-11-3p are seen) (full lists are in Supplemental Tables S2, S3). miR-34-18nt, miR-276a/b-5p-17nt, and miR-981-5p-21nt showed an extremely high R_{21} ratio at 3 d and/or 30 d (>16) (Supplemental Tables S2, S3). This suggests much higher accumulation of these miRNA isoforms in Ago2-IP compared with Ago1-IP at 3 d and/or 30 d. This could happen because of biologically relevant up-regulation of these miRNA isoforms or cloning bias and degradation from the corresponding longer isoforms. These miRNA isoforms were removed from this figure because including these data obscured the distribution of the other data in the plot. miR-34-18nt was undetectable by Ago1-IP versus Ago2-IP Northerns. Therefore, most-likely, miR-34-18nt is an artifact of library preparation. (*B*) Fold change of the main isoform of preferentially Ago2-loaded miRNA isoforms with age (30 d/3 d). Red indicates miRNAs known from our Northern analyses that show an increase in Ago2 association with age. Black arrows here and green bars in Supplemental Figure 4 indicate abundant miRNAs that were tested for accumulation in Ago2 with age in *C*. (*C*) Northern analysis (*top*) and quantitation (*bottom*) of miRNAs highlighted by the analyses in *B* and Supplemental Figure 4.
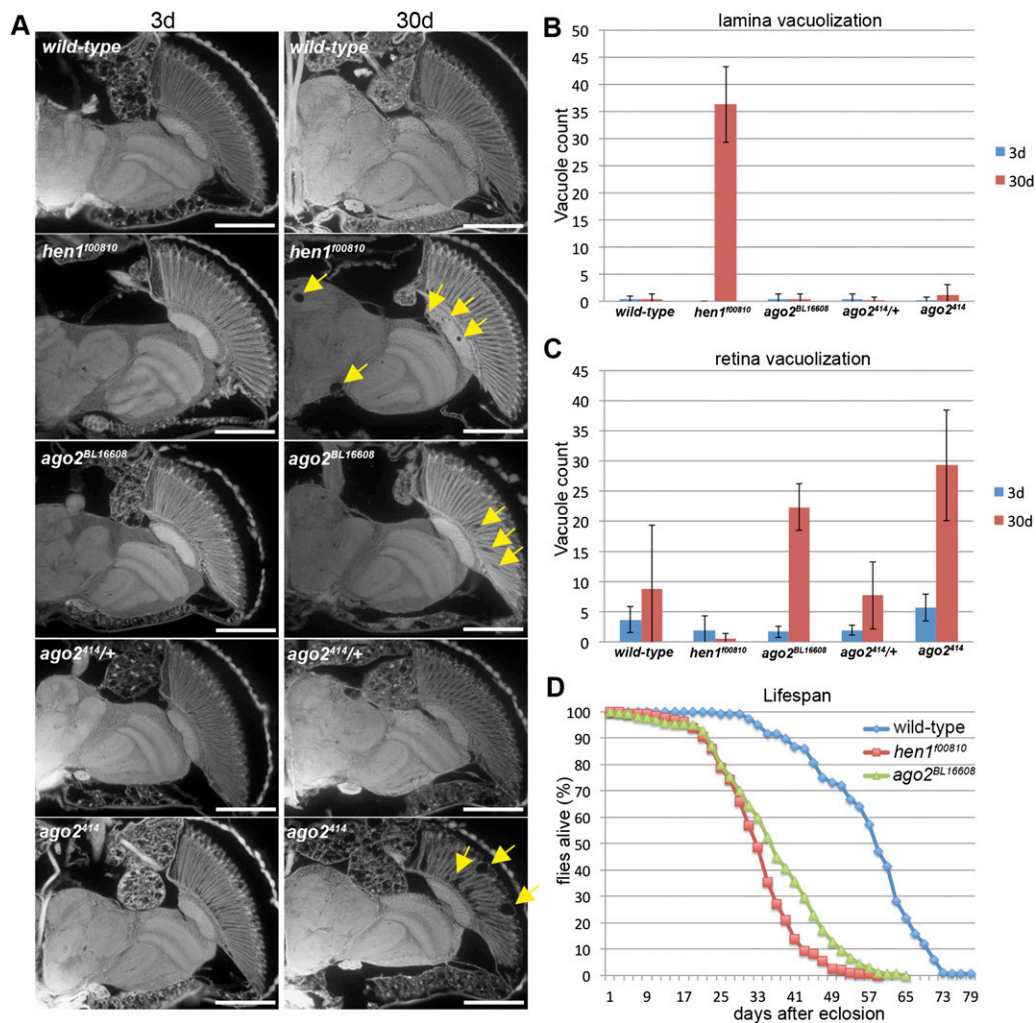
Figure 7. Mutations in *Hen1* and *Ago2* are associated with age-dependent brain degeneration and shorter life span. (*A*) Paraffin sections of wild-type, *Hen1^f00810^*, *Ago2^BL16608^*, *Ago2^414^*/+, and *Ago2^414^* heads at 3 d and 30 d. Bar, 0.1 mm. The abundant vacuoles that are present in 30-d animals in the mutants are highlighted in yellow. (*B*) Quantification of brain vacuoles in lamina. (*C*) Quantification of brain vacuoles in retina. (*D*) Life span of wild-type, *Hen1^f00810^*, and *Ago2^BL16608^* mutants. Mutant lines have been backcrossed into the genetic background of the control wild type (see the Materials and Methods). The life spans of the mutants are significantly different from wild type. $P < 0.0001$ for each compared with wild type; log rank analysis; χ^2 value with *Hen1^f00810^* is 327.7; χ^2 value with *Ago2^BL16608^* is 253.3.

small RNAs, one class of which is miRNAs, is critical for age-associated processes in *Drosophila*.

Discussion

Dynamic regulation of Ago1 vs. Ago2 loading of miRNAs with age

Increasing evidence suggests that miRNAs show heterogeneity at the 5′ end and 3′ end and even in precise sequence in different cell types and biological contexts (Neilsen et al. 2012). Despite this, it is less understood whether and how such heterogeneity is regulated biologically or its biological impact. Here, by examining the age-associated pattern of miRNA isoforms, we show that 2′-*O*-methylation of miRNAs changes in an age-depen-

dent manner in *Drosophila*. This change is correlated with a shift in partitioning of miRNAs into Ago2 versus Ago1 with age. These data suggest that the partitioning of miRNAs between Ago1 and Ago2 is modulated with age in *Drosophila*.

The mechanism of miRNA loading into the different Ago complexes in *Drosophila*, especially in vivo, remains unclear. Previously, miR-277 was shown to be loaded into both Ago1 and Ago2 because of the lack of an extensive central bulge in the miR-277/miR-277* duplex (Forstemann et al. 2007). However, our analysis of the miRNAs that show higher levels of 2′-*O*-methylation with age failed to identify a consistent lack of central bulges on miRNA/miRNA* duplexes (Supplemental Fig. S5). Rather, our results indicate that miRNA isoforms with the same sequence and length can be partitioned into both Ago1 and Ago2 and

that a change in this distribution is an age-associated phenomenon. This effect, at least in vivo, is likely to be driven by a bulge-independent mechanism. Bulge-independent partitioning of small RNAs into different Ago complexes is suggested from other studies as well: The loop sequence from miR-34 precursor stem–loop is abundant in some cells and loaded into Ago1 despite its single-stranded nature (Okamura et al. 2013).

In vivo significance of differential partitioning of miRNAs between Ago1 and Ago2 with age

Our analyses of *Hen1* and *Ago2* mutants suggest that 2′-*O*-methylation of small RNAs affects age-associated traits of brain degeneration and life span. In addition to effects on other small RNA classes, it is possible that the loss of 2′-*O*-methylation of miRNAs leads to destabilization of the miRNAs, thus affecting target silencing and contributing to accelerated age-associated defects. In this case, Ago2-loaded, but not Ago1-loaded, miRNAs would be selectively affected. Interestingly, both Ago1 and Ago2 are active in silencing miRNA targets. However, *Drosophila* Ago1 and Ago2 use different mechanisms to silence target mRNAs, as silencing by let-7 Ago1-RISC entails the removal of the polyA tail, whereas that by let-7 Ago2-RISC entails retention of the polyA tail (Iwasaki et al. 2009). Such mechanistic differences might contribute to the differential silencing efficiency of the two Ago complexes of the reporters: let-7 Ago1-RISC is more efficient than let-7 Ago2-RISC in silencing the reporters (Iwasaki et al. 2009). Our analysis of gene expression changes with age indicates a global down-regulation in the brain; correlating this with Ago1 versus Ago2 knockdown data in cells indicates greater down-regulation of predicted mRNA targets of miRNAs shifted to Ago2. While we cannot exclude that such changes result from other activities of Ago2 (Taliaferro et al. 2013), the observed reversal of expression is also consistent with a model of regulation resulting from increased loading of miRNAs shifted to Ago2 with age. Thus, potentially, the shift of these miRNAs into Ago2 may affect down-regulation of their targets with age, and disruption of this process in *Hen1* and *Ago2* mutants, along with effects on other small RNAs, may contribute to the life span and neurodegenerative phenotypes observed. Further experimental testing of the effects on mRNA targets by the miRNAs when loaded into Ago1 versus Ago2 may reveal specific details regarding the functional effects of the partitioning of the miRNAs between the RISCs and the biological outcomes.

An interesting possibility is that, by shifting miRNAs toward Ago2 from Ago1 with age, the organism might be adjusting the efficiency of target gene expression for ongoing or upcoming age-associated stresses. Since Ago2-mediated translational silencing causes retention of the polyA tail (Iwasaki et al. 2009), this might make it possible to respond to age-associated internal or external stresses more rapidly by reactivation of target mRNAs. Another possibility is the effect of loss of 2′-*O*-methylation on other classes of small RNAs, such as endo-siRNAs or

piRNAs (Horwich et al. 2007; Czech et al. 2008; Ghildiyal et al. 2008; Kawamura et al. 2008; Okamura et al. 2008). Loss of *Ago2* leads to decreased production of endo-siRNAs, which is correlated with up-regulation of transposons (Czech et al. 2008; Ghildiyal et al. 2008; Kawamura et al. 2008; Okamura et al. 2008). Recently, an age-associated increase of transposon expression and shorter life span were noted in *Ago2* mutants (Li et al. 2013). Although *Ago2* mutants show developmental defects (Pepper et al. 2009), both *Hen1[f00810]* and *Ago2* mutants are maintained in homozygous condition, and the overall brain morphology and climbing activity of these mutants when young are normal (see Fig. 7). Although it is possible that loss of these gene activities during development might sensitize the adult state, taken together, these data suggest that the defects observed in adult *Hen1* and *Ago2* mutants more likely reflect defects in adult age-associated processes. These findings support the importance of terminal modification of small RNAs on impacting age-associated traits.

Dynamic miRNA isoform regulation with age

It has become evident that the pattern of miRNA isoforms varies in different biological contexts, such as different stages of development, different tissues, and disease (Fernandez-Valverde et al. 2010; Marti et al. 2010; Li et al. 2012; Neilsen et al. 2012; Llorens et al. 2013). It is also becoming evident that such isoform distributions are regulated (Neilsen et al. 2012). For example, Nbr defines the 3′ end of many *Drosophila* miRNAs (Han et al. 2011; Liu et al. 2011), and Loqs-PB (*Drosophila* homolog of TRBP) partnering with Dcr-1 defines the cleavage position of several *Drosophila* miRNAs, which seems conserved in mammals as well (Fukunaga et al. 2012; Lee and Doudna 2012). Our study reveals another repertoire of biological heterogeneity of miRNAs: differential 2′-*O*-methylation of miRNA with age. It is intriguing that the loss of such miRNA heterogeneity leads to clear biological defects (M Abe and N Bonini, unpubl.; this study). These results raise the possibility that, in the aging adult, fine-tuning of miRNA heterogeneity might be critical for combating age-associated stresses.

Materials and methods

Small RNA Northern hybridization

Total RNA was extracted from fly tissues using Trizol reagent (#15596-018, Life Technologies) following the manufacturer's protocol. Three micrograms to ∼10 μg of total RNA was loaded per lane in 15% TBE-urea gel (#EC6885BOX, Life Technologies) and then transferred to nylon membrane (Hybond N+, GE Healthcare). After UV cross-linking and prehybridization (1 h at 50°C), the membranes were hybridized with P[32]-labeled probes overnight at 50°C. DNA oligonucleotides were annealed to obtain the templates for RNA probes. The sequences of the DNA oligonucleotides used to make probes were miR-34-5p (5′-GATAATACGACTCACTATAGGGAGA-3′/5′-AAAAAATGGCAGTGTGGTTAGCTGGTTGTGTCTCCCTATAGTGAGTCGTATTATC-3′), miR-263a-5p (5′-GATAATACGACTCACTATAGGGAGA-3′/5′-GTTAATGGCACTGGAAGAATTCACTCTC

CCTATAGTGAGTCGTATTATC-3′), miR-305-5p (5′-GATAA
TACGACTCACTATAGGGAGA-3′/5′-AAAAAAATTGTACTTC
ATCAGGTGCTCTGTCTCCCTATAGTGAGTCGTATTATC-
3′), miR-317-3p (5′-GATAATACGACTCACTATAGGGAGA-3′/
5′-AAAAAAATGAACACAGCTGGTGGTATCCAGTTCTCCCT
ATAGTGAGTCGTATTATC-3′), esi2.1 (5′-GATAATACGACTC
ACTATAGGGAGA-3′/5′-TTGACTCCAACAAGTTCGCTCCTC
TCCCTATAGTGAGTCGTATTATC-3′), miR-8 (5′-GATAATAC
GACTCACTATAGGGAGA-3′/5′-AAAAAATAATACTGTCAGG
TAAAGATGTTCTCCCTATAGTGAGTCGTATTATC-3′), miR-
100 (5′-AAAAAAAACCCGTAAATCCGAACTTGTGTCTCCC
TATAGTGAGTCGTATTATC-3′), miR-1000 (5′-GATAATACG
ACTCACTATAGGGAGA-3′/5′-AAAAAAATATTGTCCTGTCA
CAGCAGTTCTCCCTATAGTGAGTCGTATTATC-3′), and 2S
rRNA (5′-GATAATACGACTCACTATAGGGAGA-3′/5′-TGC
TTGACTACATATGGTTGAGGGTTGTATCTCCCTATAGTG
AGTCGTATTAT C-3′). P^{32}-labeled probes were synthesized by
in vitro transcription using MAXIscript T7 kit (#AM1312, Life
Technologies), supplemented with P^{32}-α-UTP.

Oxidation/β-elimination of RNA

Total RNA was extracted from fly tissues using Trizol reagent
(#15596-018, Life Technologies) following the manufacturer's
protocol. Total RNA was resuspended in 1× borate/borax buffer
with or without $NaIO_4$ (final concentration 25 mM) (#311448,
Sigma-Aldrich) and incubated for 30 min at room temperature in
the dark. After adding 1/10 vol of 100% glycerol, the samples
were incubated further for 10 min at room temperature in the
dark. After purifying the RNA, the RNA samples were resus-
pended in 1× borate/borax buffer and supplemented with NaOH
to a final concentration of 0.1 mM. The samples were incubated
for 90 min at 45°C followed by purification and analysis by
Northern blots. Ten micrograms to ~20 µg of total RNA was
used for each miRNA.

IP-Northern

Fly lysate was prepared from 3-d and 30-d male Flag-HA-Ago2
whole flies (Czech et al. 2008). Approximately 80 flies were used
for each IP (Ago1 or Ago2) followed by Northerns (miR-34-5p,
esi-2.1, miR-305-5p, miR-263a-5p, miR-11-3p, and miR-317-3p).
Immunoprecipitation was performed as described (Kirino et al.
2011), except that 800 mM NaCl (final concentration) was used
for Ago2-IP. Anti-Ago1 (ab5070, Abcam) and M2 beads (#A2220,
Sigma-Aldrich) were used for Ago1 and Ago2-IP, respectively.
After extraction of RNA from beads as described in Kirino et al.
(2011), the purified RNA was loaded onto 15% TBE-urea gel
followed by Northern blots.

Preparation of Ago1 and Ago2-IP small RNA libraries

Forty whole male flies (Flag-HA-Ago2, 3 d and 30 d) were used for
Ago1-IP, and 200 whole male flies (3 d and 30 d) were used for
Ago2 (M2)-IP. After immunoprecipitation of Ago1 or Ago2, the
purified RNA was P^{32}-labeled as described (Kirino et al. 2011),
and the radiolabeled RNA was run on a 15% TBE-urea gel
(#EC6885BOX, Life Technologies). The gel was exposed to
a PhosphorImager screen, and the fractions corresponding to
small RNAs were excised from the gel. After purifying the
small RNAs from the gel, small RNA libraries were generated
using Illumina's TruSeq small RNA sample preparation kit
(#RS-200-0012, Illumina, Inc.) following the manufacturer's
protocol. The libraries were sequenced on a HiSeq2000 plat-
form (Illumina).

Western immunoblots

Fly tissues were resuspended in RIPA buffer followed by grinding
and centrifugation to remove debris. The supernatant was mea-
sured by Bradford assay, and 25~50 µg of protein was loaded onto
each lane. NuPAGE Novex 4%–12% Bis-Tris gel (#NP0321BOX,
Life Technologies) was used to run the samples in 1× NuPAGE
MES SDS running buffer (#NP0002, Life Technologies). Proteins
were transferred to PVDF membrane, and the membrane was
blocked by 5% milk/TBST for 1 h at 4°C. The membrane was
incubated with primary antibody overnight at 4°C. After washing
the membrane in TBST buffer three times (5 min each), the
membrane was incubated with secondary antibody for 2 h at 4°C.
The membrane was washed in TBST three times (5 min each)
followed by signal development by Pierce ECL plus Western
blotting substrate (#32132, Thermo Fisher Scientific). The image
was scanned by a Fujifilm LAS-3000 Imager (Fujifilm). For Ago2
Western, Flag-HA-Ago2 male flies were used. For R2D2 and Dcr2
Western blot, wild-type male flies were used. The primary
antibodies used were anti-Flag-HRP (1:2000; #A8592, Sigma-
Aldrich) for Ago2. Anti-Ago1 (1:500–1:1000) for Westerns was
a kind gift of the Mourelatos laboratory. Anti-R2D2 (rabbit poly-
clonal) and anit-Dcr2 (mouse monoclonal) antibodies were kind
gifts from the Siomi laboratory. Anti-Actin Ab (Ab8227, Abcam)
was used at 1:2000. The secondary antibodies used were anti-
mouse IgG-HRP (1:2000; #7076S, Cell Signaling Technology, Inc.)
and anti-rabbit IgG-HRP (1:2000; #sc-2030, Santa Cruz Biotech-
nology, Inc.).

Fly stocks

Flies were grown in standard cornmeal molasses agar medium at
25°C. Hen1^{f00810} (FlyBase ID: FBst1016506, The Exelixis Collec-
tion at the Harvard Medical School) and Ago2^{414} (FlyBase ID:
FBst0313641, Drosophila Genetic Resource Center, Kyoto Stock
Center) flies were kind gifts from the Sara Cherry laboratory.
Ago2^{BL16608} (FlyBase ID: FBst0016608) and Flag-HA-Ago2 flies
(FlyBase ID: FBst0033242) were obtained from the Bloomington
Stock Center. Hen1^{f00810} and Ago2^{BL16608} lines were backcrossed
into a homogenous wild-type background (Bloomington Stock
Line 5905 [BL5905], FlyBaseID: FBst0005905, w^{1118}) for five
generations.

Life span assay

One-hundred-eighty to ~200 flies were used for each life span
replicate. Male flies were collected on the day of eclosion (15 flies
per vial), aged at 25°C, and transferred to new fly food vials every
other day while scored for survival. The assay was repeated in
triplicate and was analyzed by Excel (Microsoft) and GraphPad
Prism for survival curves.

Brain paraffin sections

Adult female heads (3 d and 30 d) were used for paraffin sections
as described (Li et al. 2008). Brain vacuoles were counted for
lamina or retina through 10 continuous horizontal sections,
defining the center section, with esophagus being most prom-
inent. Four heads per genotype were used for quantification.

Computational analyses

Mapping and histograms Adaptor sequences were removed
from the 3′ ends of the reads in the Illumina fastQ-generated files
using the fastx toolkit (http://hannonlab.cshl.edu/fastx_toolkit).
The adapter sequences were as follows: 5′ adapter, 5′-GUUCA-

GAGUUCUACAGUCCGACGAUC-3′; and 3′ adapter, 5′-TGG AATTCTCGGGGTGCCAAGG-3′.

Reads were then collapsed and annotated with the number of times each was sequenced, and only unique reads were analyzed. Reads were filtered based on base-pair size such that reads <16 base pairs (bp) or >30 bp were discarded. The remaining reads were then mapped using Bowtie to the *Drosophila melanogaster* (*dm5*) genome and miRNA stem–loop sequences obtained from miRBase (release 20). Bowtie parameters were restricted to output only perfectly aligned matches to the stem–loop sequence. The reads were aligned and mapped to entire miRNA stem–loops. After aligning, each read was annotated as either a 5P or a 3P. To do this, the stem–loop sequence was split in half, with the first half designated the 5′ arm and the second half designated the 3′ arm, as the start and end positions of most miRNAs are imprecise.

Change in the read number and percentage of total miRNAs and other classes of small RNAs   All processed reads were first mapped to transposons annotated by FlyBase (ftp://ftp.flybase.net/ genomes/Drosophila_melanogaster/current/fasta). The rest of the reads were stored and mapped to miRNA stem–loop regions as well as known ncRNAs (snRNAs, snoRNAs, tRNAs, and rRNAs) and the rest of the genome (defined as "ncRNA" and "genome" by FlyBase).

Identification of preferentially Ago2-loaded miRNA isoforms at 3 d and 30 d   We identified miRNA isoforms preferentially loaded into Ago2 compared with Ago1 for flies of different ages using a measure of "Ago2/Ago1 relative load ratio" or R_{21}. The most abundant isoform from each miRNA stem (5p or 3p) from the Ago2-IP 3-d library was selected. For all of the isoforms in each library that start with the same 5′ nucleotide position, we denoted the share of each isoform s_i^{lib} such that $\sum_i s_i^{lib} = 1$ in each library and denoted the share of the most abundant isoform S^{lib}. The age ratio for 3-d flies was $R^{3d}_{21} = S^{3dAgo2}/S^{3dAgo1}$ (*X*-axis in Fig. 6A), and the age ratio for 30-d flies was $R^{30d}_{21} = S^{30dAgo2}/S^{30dAgo1}$ (*Y*-axis in Fig. 6A). 5p and 3p miRNA stem sequences were classified as "mature" and "star" based on their relative (high and low, respectively) deep sequencing read counts in the Ago1 sample at 3 d (strand with S^{3dAgo1} being the mature strand). To compare the ratio of a specific isoform between Ago1 and Ago2, after assigning to the "mature" or "star" category, we kept only the cases with the mature and star categories consistent among all four libraries. Thus, if there was a discrepancy of the relatively more abundant stem (5p or 3p) between Ago1-3d and any of the other three libraries (Ago2-3d, Ago1-30d, and Ago2-30d), those cases were removed. This was to assure that the same isoform was consistently called "mature" or "star" in all four libraries (Ago1-3d, Ago1-30d, Ago2-3d, and Ago2-30d). We also filtered out any miRNAs that were below a 1000 read count threshold. Note that miR-34-18nt, miR-276a/b-5p-17nt, and miR-981-5p-21nt showed an extremely high R_{21} ratio at 3 d and/or 30 d (>16) (Supplemental Tables S2, S3). This suggests much higher accumulation of these miRNA isoforms in Ago2-IP compared with Ago1-IP at 3 d and/or 30 d. This could happen due to either biologically relevant up-regulation of these miRNA isoforms or cloning bias or degradation from the corresponding longer isoforms. These miRNA isoforms were removed from Figure 6 because including the dots corresponding to these miRNA isoforms obscured the distribution of the other dots in the plot (see Fig. 6A). miR-34-18nt was undetectable by Ago1 versus Ago2-IP Northerns; therefore, most likely, miR-34–18nt is an abnormal by-product of the library preparation. After identifying preferentially loaded Ago2 isoforms, we calculated a ratio of normalized reads at 30 d and 3 d for each specific isoform. The ratios (fold change) were plotted as in Figure 6B. To check for selective enrichment of particular miRNAs from the data of Ghildiyal et al. (2010), we first identified the most abundant isoform for each miRNA in the total RNA set (GSM466487). For each of the libraries (GSM466488 and GSM466489), we counted the number of reads (M) for these isoforms and calculated their relative enrichment as $E = N/(N − M)$, where N is the total number of library reads for a given miRNA. We then plotted the enrichment ratio $E_{GSM466488}/E_{GSM466489}$ in Supplemental Figure 4. Note that we used both sequence analysis for discovery of new Ago2 preferentially loaded miRNAs (see Fig. 6A,B; Supplemental Fig. 4) and Northern analysis (see Fig. 6C), as each technique (deep sequencing and Northern analysis) will have strengths and weaknesses. The Gene Expression Omnibus record for libraries generated here is GSE52963. We also analyzed previously published microarray data GSE25009 from Liu et al. (2012) and data from Taliaferro et al. (2013).

References

Alon S, Mor E, Vigneault F, Church GM, Locatelli F, Galeano F, Gallo A, Shomron N, Eisenberg E. 2012. Systematic identification of edited microRNAs in the human brain. *Genome Res* **22**: 1533–1540.

Ameres SL, Horwich MD, Hung JH, Xu J, Ghildiyal M, Weng Z, Zamore PD. 2010. Target RNA-directed trimming and tailing of small silencing RNAs. *Science* **328**: 1534–1539.

Azuma-Mukai A, Oguri H, Mituyama T, Qian ZR, Asai K, Siomi H, Siomi MC. 2008. Characterization of endogenous human Argonautes and their miRNA partners in RNA silencing. *Proc Natl Acad Sci* **105**: 7964–7969.

Bartel DP. 2004. MicroRNAs: Genomics, biogenesis, mechanism, and function. *Cell* **116**: 281–297.

Boehm M, Slack F. 2005. A developmental timing microRNA and its target regulate life span in *C. elegans*. *Science* **310**: 1954–1957.

Burroughs AM, Ando Y, de Hoon MJ, Tomaru Y, Nishibu T, Ukekawa R, Funakoshi T, Kurokawa T, Suzuki H, Hayashizaki Y, et al. 2010. A comprehensive survey of 3′ animal miRNA modification events and a possible role for 3′ adenylation in modulating miRNA targeting effectiveness. *Genome Res* **20**: 1398–1410.

Calabrese JM, Seila AC, Yeo GW, Sharp PA. 2007. RNA sequence analysis defines Dicer's role in mouse embryonic stem cells. *Proc Natl Acad Sci* **104**: 18097–18102.

Czech B, Malone CD, Zhou R, Stark A, Schlingeheyde C, Dus M, Perrimon N, Kellis M, Wohlschlegel JA, Sachidanandam R, et al. 2008. An endogenous small interfering RNA pathway in *Drosophila*. *Nature* **453**: 798–802.

Czech B, Zhou R, Erlich Y, Brennecke J, Binari R, Villalta C, Gordon A, Perrimon N, Hannon GJ. 2009. Hierarchical rules for Argonaute loading in *Drosophila*. *Mol Cell* **36**: 445–456.

de Lencastre A, Pincus Z, Zhou K, Kato M, Lee SS, Slack FJ. 2010. MicroRNAs both promote and antagonize longevity in *C. elegans*. *Curr Biol* **20**: 2159–2168.

Ekdahl Y, Farahani HS, Behm M, Lagergren J, Ohman M. 2012. A-to-I editing of microRNAs in the mammalian brain increases during development. *Genome Res* **22**: 1477–1487.

Fernandez-Valverde SL, Taft RJ, Mattick JS. 2010. Dynamic isomiR regulation in *Drosophila* development. *RNA* **16:** 1881–1888.

Forstemann K, Horwich MD, Wee L, Tomari Y, Zamore PD. 2007. *Drosophila* microRNAs are sorted into functionally distinct argonaute complexes after production by dicer-1. *Cell* **130:** 287–297.

Fukunaga R, Han BW, Hung JH, Xu J, Weng Z, Zamore PD. 2012. Dicer partner proteins tune the length of mature miRNAs in flies and mammals. *Cell* **151:** 533–546.

Ghildiyal M, Seitz H, Horwich MD, Li C, Du T, Lee S, Xu J, Kittler EL, Zapp ML, Weng Z, et al. 2008. Endogenous siRNAs derived from transposons and mRNAs in *Drosophila* somatic cells. *Science* **320:** 1077–1081.

Ghildiyal M, Xu J, Seitz H, Weng Z, Zamore PD. 2010. Sorting of *Drosophila* small silencing RNAs partitions microRNA* strands into the RNA interference pathway. *RNA* **16:** 43–56.

Han BW, Hung JH, Weng Z, Zamore PD, Ameres SL. 2011. The 3′-to-5′ exoribonuclease Nibbler shapes the 3′ ends of microRNAs bound to *Drosophila* Argonaute1. *Curr Biol* **21:** 1878–1887.

Horwich MD, Li C, Matranga C, Vagin V, Farley G, Wang P, Zamore PD. 2007. The *Drosophila* RNA methyltransferase, DmHen1, modifies germline piRNAs and single-stranded siRNAs in RISC. *Curr Biol* **17:** 1265–1272.

Hutvagner G, McLachlan J, Pasquinelli AE, Balint E, Tuschl T, Zamore PD. 2001. A cellular function for the RNA-interference enzyme Dicer in the maturation of the let-7 small temporal RNA. *Science* **293:** 834–838.

Ibanez-Ventoso C, Yang M, Guo S, Robins H, Padgett RW, Driscoll M. 2006. Modulated microRNA expression during adult lifespan in *Caenorhabditis elegans*. *Aging Cell* **5:** 235–246.

Iki T, Yoshikawa M, Nishikiori M, Jaudal MC, Matsumoto-Yokoyama E, Mitsuhara I, Meshi T, Ishikawa M. 2010. In vitro assembly of plant RNA-induced silencing complexes facilitated by molecular chaperone HSP90. *Mol Cell* **39:** 282–291.

Iwasaki S, Kawamata T, Tomari Y. 2009. *Drosophila* argonaute1 and argonaute2 employ distinct mechanisms for translational repression. *Mol Cell* **34:** 58–67.

Iwasaki S, Kobayashi M, Yoda M, Sakaguchi Y, Katsuma S, Suzuki T, Tomari Y. 2010. Hsc70/Hsp90 chaperone machinery mediates ATP-dependent RISC loading of small RNA duplexes. *Mol Cell* **39:** 292–299.

Kamminga LM, Luteijn MJ, den Broeder MJ, Redl S, Kaaij LJ, Roovers EF, Ladurner P, Berezikov E, Ketting RF. 2010. Hen1 is required for oocyte development and piRNA stability in zebrafish. *EMBO J* **29:** 3688–3700.

Kato M, Chen X, Inukai S, Zhao H, Slack FJ. 2011. Age-associated changes in expression of small, noncoding RNAs, including microRNAs, in *C. elegans*. *RNA* **17:** 1804–1820.

Kawahara Y, Zinshteyn B, Sethupathy P, Iizasa H, Hatzigeorgiou AG, Nishikura K. 2007. Redirection of silencing targets by adenosine-to-inosine editing of miRNAs. *Science* **315:** 1137–1140.

Kawamura Y, Saito K, Kin T, Ono Y, Asai K, Sunohara T, Okada TN, Siomi MC, Siomi H. 2008. *Drosophila* endogenous small RNAs bind to Argonaute 2 in somatic cells. *Nature* **453:** 793–797.

Kenyon C. 2010. A pathway that links reproductive status to lifespan in *Caenorhabditis elegans*. *Ann N Y Acad Sci* **1204:** 156–162.

Kirino Y, Mourelatos Z. 2007a. 2′-*O*-methyl modification in mouse piRNAs and its methylase. *Nucleic Acids Symp Ser (Oxf)* **51:** 417–418.

Kirino Y, Mourelatos Z. 2007b. The mouse homolog of HEN1 is a potential methylase for Piwi-interacting RNAs. *RNA* **13:** 1397–1401.

Kirino Y, Mourelatos Z. 2007c. Mouse Piwi-interacting RNAs are 2′-*O*-methylated at their 3′ termini. *Nat Struct Mol Biol* **14:** 347–348.

Kirino Y, Vourekas A, Khandros E, Mourelatos Z. 2011. Immunoprecipitation of piRNPs and directional, next generation sequencing of piRNAs. *Methods Mol Biol* **725:** 281–293.

Kurth HM, Mochizuki K. 2009. 2′-*O*-methylation stabilizes Piwi-associated small RNAs and ensures DNA elimination in *Tetrahymena*. *RNA* **15:** 675–685.

Landgraf P, Rusu M, Sheridan R, Sewer A, Iovino N, Aravin A, Pfeffer S, Rice A, Kamphorst AO, Landthaler M, et al. 2007. A mammalian microRNA expression atlas based on small RNA library sequencing. *Cell* **129:** 1401–1414.

Lee HY, Doudna JA. 2012. TRBP alters human precursor microRNA processing in vitro. *RNA* **18:** 2012–2019.

Lee RC, Feinbaum RL, Ambros V. 1993. The *C. elegans* heterochronic gene lin-4 encodes small RNAs with antisense complementarity to lin-14. *Cell* **75:** 843–854.

Li J, Yang Z, Yu B, Liu J, Chen X. 2005. Methylation protects miRNAs and siRNAs from a 3′-end uridylation activity in *Arabidopsis*. *Curr Biol* **15:** 1501–1507.

Li LB, Yu Z, Teng X, Bonini NM. 2008. RNA toxicity is a component of ataxin-3 degeneration in *Drosophila*. *Nature* **453:** 1107–1111.

Li SC, Liao YL, Ho MR, Tsai KW, Lai CH, Lin WC. 2012. miRNA arm selection and isomiR distribution in gastric cancer. *BMC Genomics* **13:** S13.

Li W, Prazak L, Chatterjee N, Gruninger S, Krug L, Theodorou D, Dubnau J. 2013. Activation of transposable elements during aging and neuronal decline in *Drosophila*. *Nat Neurosci* **16:** 529–531.

Liu Q, Rand TA, Kalidas S, Du F, Kim HE, Smith DP, Wang X. 2003. R2D2, a bridge between the initiation and effector steps of the *Drosophila* RNAi pathway. *Science* **301:** 1921–1925.

Liu N, Abe M, Sabin LR, Hendriks GJ, Naqvi AS, Yu Z, Cherry S, Bonini NM. 2011. The exoribonuclease Nibbler controls 3′ end processing of microRNAs in *Drosophila*. *Curr Biol* **21:** 1888–1893.

Liu N, Landreh M, Cao K, Abe M, Hendriks GJ, Kennerdell JR, Zhu Y, Wang LS, Bonini NM. 2012. The microRNA miR-34 modulates ageing and neurodegeneration in *Drosophila*. *Nature* **482:** 519–523.

Llorens F, Hummel M, Pantano L, Pastor X, Vivancos A, Castillo E, Matllin H, Ferrer A, Ingham M, Noguera M, et al. 2013. Microarray and deep sequencing cross-platform analysis of the mirRNome and isomiR variation in response to epidermal growth factor. *BMC Genomics* **14:** 371.

Marques JT, Kim K, Wu PH, Alleyne TM, Jafari N, Carthew RW. 2010. Loqs and R2D2 act sequentially in the siRNA pathway in *Drosophila*. *Nat Struct Mol Biol* **17:** 24–30.

Marti E, Pantano L, Banez-Coronel M, Llorens F, Minones-Moyano E, Porta S, Sumoy L, Ferrer I, Estivill X. 2010. A myriad of miRNA variants in control and Huntington's disease brain regions detected by massively parallel sequencing. *Nucleic Acids Res* **38:** 7219–7235.

Miyoshi T, Takeuchi A, Siomi H, Siomi MC. 2010. A direct role for Hsp90 in pre-RISC formation in *Drosophila*. *Nat Struct Mol Biol* **17:** 1024–1026.

Neilsen CT, Goodall GJ, Bracken CP. 2012. IsomiRs—the overlooked repertoire in the dynamic microRNAome. *Trends Genet* **28:** 544–549.

Nishida KM, Miyoshi K, Ogino A, Miyoshi T, Siomi H, Siomi MC. 2013. Roles of R2D2, a cytoplasmic D2 body compo-

nent, in the endogenous siRNA pathway in *Drosophila*. *Mol Cell* **49:** 680–691.

Nishikura K. 2010. Functions and regulation of RNA editing by ADAR deaminases. *Annu Rev Biochem* **79:** 321–349.

Okamura K, Ishizuka A, Siomi H, Siomi MC. 2004. Distinct roles for Argonaute proteins in small RNA-directed RNA cleavage pathways. *Genes Dev* **18:** 1655–1666.

Okamura K, Chung WJ, Ruby JG, Guo H, Bartel DP, Lai EC. 2008. The *Drosophila* hairpin RNA pathway generates endogenous short interfering RNAs. *Nature* **453:** 803–806.

Okamura K, Liu N, Lai EC. 2009. Distinct mechanisms for microRNA strand selection by *Drosophila* Argonautes. *Mol Cell* **36:** 431–444.

Okamura K, Robine N, Liu Y, Liu Q, Lai EC. 2011. R2D2 organizes small regulatory RNA pathways in *Drosophila*. *Mol Cell Biol* **31:** 884–896.

Okamura K, Ladewig E, Zhou L, Lai EC. 2013. Functional small RNAs are generated from select miRNA hairpin loops in flies and mammals. *Genes Dev* **27:** 778–792.

Pepper AS, Beerman RW, Bhogal B, Jongens TA. 2009. Argonaute2 suppresses *Drosophila* fragile X expression preventing neurogenesis and oogenesis defects. *PLoS ONE* **4:** e7618.

Reinhart BJ, Slack FJ, Basson M, Pasquinelli AE, Bettinger JC, Rougvie AE, Horvitz HR, Ruvkun G. 2000. The 21-nucleotide let-7 RNA regulates developmental timing in *Caenorhabditis elegans*. *Nature* **403:** 901–906.

Ren G, Chen X, Yu B. 2012. Uridylation of miRNAs by hen1 suppressor1 in *Arabidopsis*. *Curr Biol* **22:** 695–700.

Ruby JG, Jan C, Player C, Axtell MJ, Lee W, Nusbaum C, Ge H, Bartel DP. 2006. Large-scale sequencing reveals 21U-RNAs and additional microRNAs and endogenous siRNAs in *C. elegans*. *Cell* **127:** 1193–1207.

Seitz H, Ghildiyal M, Zamore PD. 2008. Argonaute loading improves the 5′ precision of both MicroRNAs and their miRNA* strands in flies. *Curr Biol* **18:** 147–151.

Smith-Vikos T, Slack FJ. 2012. MicroRNAs and their roles in aging. *J Cell Sci* **125:** 7–17.

Taliaferro JM, Aspden JL, Bradley T, Marwha D, Blanchette M, Rio DC. 2013. Two new and distinct roles for *Drosophila* Argonaute-2 in the nucleus: Alternative pre-mRNA splicing and transcriptional repression. *Genes Dev* **27:** 378–389.

Tomari Y, Matranga C, Haley B, Martinez N, Zamore PD. 2004. A protein sensor for siRNA asymmetry. *Science* **306:** 1377–1380.

Tomari Y, Du T, Zamore PD. 2007. Sorting of *Drosophila* small silencing RNAs. *Cell* **130:** 299–308.

Vagin VV, Sigova A, Li C, Seitz H, Gvozdev V, Zamore PD. 2006. A distinct small RNA pathway silences selfish genetic elements in the germline. *Science* **313:** 320–324.

Westholm JO, Ladewig E, Okamura K, Robine N, Lai EC. 2012. Common and distinct patterns of terminal modifications to mirtrons and canonical microRNAs. *RNA* **18:** 177–192.

Wyman SK, Knouf EC, Parkin RK, Fritz BR, Lin DW, Dennis LM, Krouse MA, Webster PJ, Tewari M. 2011. Post-transcriptional generation of miRNA variants by multiple nucleotidyl transferases contributes to miRNA transcriptome complexity. *Genome Res* **21:** 1450–1461.

Yu B, Yang Z, Li J, Minakhina S, Yang M, Padgett RW, Steward R, Chen X. 2005. Methylation as a crucial step in plant microRNA biogenesis. *Science* **307:** 932–935.

Zhao Y, Mo B, Chen X. 2012a. Mechanisms that impact microRNA stability in plants. *RNA Biol* **9:** 1218–1223.

Zhao Y, Yu Y, Zhai J, Ramachandran V, Dinh TT, Meyers BC, Mo B, Chen X. 2012b. The *Arabidopsis* nucleotidyl transferase HESO1 uridylates unmethylated small RNAs to trigger their degradation. *Curr Biol* **22:** 689–694.